

1 **Optimisation of SARS-CoV-2 culture from clinical samples for** 2 **clinical trial applications**

3 Dominic Wooding^{1^}, Kate Buist^{1^}, Alessandra Romero-Ramirez^{1^}, Helen Savage², Rachel
4 Watkins¹, Daisy Bengey¹, Caitlin Greenland-Bews¹, Caitlin R Thompson¹, Nadia Kontogianni¹,
5 Richard Body³, Gail Hayward⁴, Rachel L Byrne², Susan Gould¹, CONDOR Steering Group³,
6 Christopher Myerscough¹, Barry Atkinson⁶, Victoria Shaw⁵, Bill Greenhalf⁵, Emily Adams¹, Ana
7 Cubas-Atienzar¹, Saye Khoo^{5,7}, Tom Fletcher^{2,7}, Thomas Edwards^{1*}.

8 [^]Joint first author, contributed equally

9 *Corresponding Author

10 Affiliations:

11 ¹Centre for Drugs and Diagnostics, Liverpool School of Tropical Medicine and Hygiene,
12 Liverpool, United Kingdom.

13 ²Department of Clinical Sciences, Liverpool School of Tropical Medicine and Hygiene,
14 Liverpool, UK.

15 ³Manchester University NHS Foundation Trust, Research and Innovation, Manchester, UK.

16 ⁴Nuffield Department of Primary Care Health Sciences, University of Oxford, Oxford, UK.

17 ⁵University of Liverpool, Liverpool, UK.

18 ⁶Research and Evaluation, UK Health Security Agency, Porton Down, Salisbury SP4 0JG, UK.

19 ⁷NIHR Royal Liverpool and Broadgreen CRF, Liverpool University Hospitals NHS Foundation
20 Trust, Liverpool, UK.

21

22 **Abstract**

23 Clinical trials of SARS-CoV-2 therapeutics often include virological secondary endpoints to
24 compare viral clearance and viral load reduction between treatment and placebo arms. This
25 is typically achieved using RT-qPCR, which cannot differentiate replicant competent virus from
26 non-viable virus or free RNA, limiting its utility as an endpoint. Culture based methods for
27 SARS-CoV-2 exist; however, these are often insensitive and poorly standardised for use as
28 clinical trial endpoints.

29 We report optimisation of a culture-based approach evaluating three cell lines, three
30 detection methods, and key culture parameters. We show that Vero-ACE2-TMPRSS2 (VAT)
31 cells in combination with RT-qPCR of culture supernatants from the first passage provides the
32 greatest overall detection of Delta viral replication (22/32, 68.8%), being able to identify viable
33 virus in 83.3% (20/24) of clinical samples with initial Ct values <30. Likewise, we demonstrate
34 that RT-qPCR using culture supernatants from the first passage of Vero hSLAM cells provides
35 the highest overall detection of Omicron viral replication (9/31, 29%), detecting live virus in
36 39.1% (9/23) of clinical samples with initial Ct values < 25. This assessment demonstrates that
37 combining RT-qPCR with virological end point analysis has utility in clinical trials of
38 therapeutics for SARS-CoV-2; however, techniques may require optimising based on dominant
39 circulating strain.

40

41 INTRODUCTION

42 The design of COVID-19 therapeutic clinical trials and appropriate selection of viral endpoints
43 is crucial to determining treatment efficacy¹. A variety of endpoints have been identified by
44 systematic reviews of SARS-CoV-2 trial endpoints, including death, recovery, need for
45 intensive care, hospital discharge, oxygenation, critical illness assessment tools, and viral load
46 assessment¹⁻³ and often multiple secondary endpoints are selected for analysis.

47

48 The use of viral load assays as an endpoint has also underpinned the early-phase evaluation
49 of antiviral activity, such as remdesivir⁴, molnupiravir⁵ and Nirmatrelvir⁶. The gold standard
50 method for detecting and quantifying SARS-CoV-2 in clinical samples is quantitative reverse-
51 transcriptase PCR (RT-qPCR) detection of viral RNA⁷. However, RT-qPCR cannot distinguish
52 between infectious virus and non-infectious degraded RNA fragments that persist after
53 neutralisation by the immune system and, therefore, may over-estimate the presence of
54 infectious virus and under-estimate efficacy of the assessed pharmaceutical. Previous studies
55 have shown a correlation between viral load by RT-qPCR during SARS-CoV-2 infection and
56 culture positivity, with culture positivity being used as an estimate of infectiousness⁸.

57

58 Since these RNA-based detection assays do not discriminate between replication-competent
59 virus and remnants of genetic material, an alternative approach is to use viral culture as a
60 proxy for antiviral efficacy. Whilst viral culture is less sensitive than RT-qPCR, it has the
61 advantage of confirming viral infectivity and therefore transmission potential^{9,10}. Culture
62 based methods for detecting SARS-CoV-2 are not well standardised and numerous cell lines

63 and culture conditions have been reported¹¹. SARS-CoV-2 cell line susceptibility is influenced
64 by many factors including cell tropism, receptor expression levels, virus replication kinetics,
65 and the epidemiological and clinical features of the virus¹². Globally, the Vero E6 African green
66 monkey kidney cell line is commonly used as a readily available cell line that is permissive for
67 infection by many viruses. Vero E6 cells do not express all SARS-CoV-2 key surface molecules,
68 and viral entry and fusion mainly occurs via non-specific endocytic mechanisms¹³. Alternative
69 Vero cells have been modified to more closely resemble the human epithelia., e.g. Vero
70 hSLAM cells that express the human signalling lymphocytic activation molecule (SLAM)¹⁴, and
71 VAT cells - Vero E6 expressing both human angiotensin-converting enzyme 2 (ACE2), the major
72 receptor of SARS-CoV-2, and transmembrane serine protease 2 (TMPRSS2), which cleaves the
73 viral S protein priming it for cellular infection¹⁵. Both viral growth kinetics and changes to cell
74 morphology (i.e., cytopathic effects; CPE) can vary between these different cell lines thereby
75 impacting the outcome of tests used to assess culture positivity¹⁶. For example, a 2020 study
76 found that cell culture supernatants from Vero E6 cells expressing TMPRSS2 had more than
77 100 times more viral RNA copies than Vero E6 cells not expressing this protein¹⁷.

78

79 There are various methods for assessing culture positivity, including the use of microscopy to
80 detect CPE caused by viral infection¹⁸ ¹⁹, plaque assays to quantify infectious virus in the
81 culture supernatants²⁰, and RT-qPCR to detect increases in viral RNA during culture²¹.

82

83 To develop a virological endpoint for trials of SARS-CoV-2 therapeutics, it is imperative that all
84 these methodological variables are assessed with the process optimised for maximal

85 sensitivity to enable accurate determination of individuals with infection-competent SARS-
 86 CoV-2 in the nasopharynx. In this paper we describe the optimisation of a viral culture assay
 87 for detecting infectious virus with assessment of three potential detection methods and three
 88 different cell lines.

89

90 **METHODOLOGY**

91

92 **Variables and experimental design**

93 Five variables were identified for optimisation (Table 1), and within each variable a set of
 94 parameters were assessed (Fig.1). Variables were tested using samples from the United
 95 Kingdom (U.K.) Delta outbreak and, once the methodology was optimised, the procedure was
 96 assessed with samples from the Omicron BA.1 outbreak.

Variant	Clinical samples	Cell lines	Passages	Detection method
DELTA	36 UTM Samples Ct categories: <20, 21-25, 26-30, >30 + Positive samples (N=8/category) Negative samples (N=4/category)	VERO E6 VAT	3 passages	CPE Plaque assay RT-qPCR
OMICRON	47 UTM Samples Ct categories: <20, 21-25, 26-30, >30 + 31 positive samples 16 negative samples	VERO E6 h/SLAM VAT	1 passage	RT-qPCR

97

98 **Figure 1.** Experimental design for the optimisation of SARS-CoV-2 culture from clinical
99 samples. Scheme of the initial experiments performed using different parameters before the
100 optimization of detection methods using clinical samples. Samples during the Delta and
101 Omicron outbreak were cultured in Vero E6, VAT and/or Vero hSLAM for 3 days. Supernatants
102 were collected to perform RT-PCR for Delta and Omicron respectively and CPE imaging and
103 plaque assays were performed for Delta only.

104

105 **Table 1:** Parameters chosen for the optimisation of the viral culture assay. CPE = cytopathic
106 effect; RT-qPCR = quantitative reverse transcriptase PCR.

Variable	Parameters
Sample Dilution	1:20, 1:10, 1:4
Length of viral incubation post-inoculation	24, 48, 72, 96, 120 hours
Vero cell lines	E6, ACE2/TMPRSS2 (VAT), hSLAM
Detection method of viable SARS-CoV-2 virus	CPE, plaque assay, RT-qPCR
Number of viral passages in culture	Passage 1, 2, 3

107

108 1. Cell culture

109 Vero C1008 [Vero 76, clone E6, Vero E6] (ECACC 85020206) (Vero E6 cells) and Vero hSLAM
110 (ECACC 04091501) (hSLAM cells) were obtained from the European collection of
111 authenticated cell cultures (ECACC). Vero E6-ACE2-TMPRSS2 cells (VAT cells) were donated
112 from Professor Wendy Barclay (Imperial College London, UK), and their development is
113 detailed in a publication from 2021¹⁵. For the duration of the experiment, Vero E6 cells were
114 maintained in T125 cell culture flasks containing 25ml of Dulbecco's Modified Eagle Medium

115 (DMEM, Gibco, USA) plus 10% foetal bovine serum (FBS, Gibco, USA) and 1% Penicillin/
116 Streptomycin solution (Gibco, USA) (D10 media) at 37°C and 5% CO₂. VAT cells were
117 maintained as described above, with a modified growth medium: DMEM plus 10% FBS, 2%
118 50mg/ml Geneticin (Gibco, USA), 1% 100X Non-essential Amino Acids (ThermoFisher, USA),
119 and 0.4% 50mg/ml Hygromycin B (Invitrogen, USA)). hSLAM cells were maintained as above
120 but with the following growth medium: Minimum Essential Media GlutaMAX™ (MEM, Gibco,
121 USA) plus 10% FBS and 2% 50mg/ml Geneticin. Adjustments in the FBS content of these
122 maintenance media to 4% (D4 media) or 2% (D2 media) were required at various points in the
123 culture process, detailed below. Once cells reached 100% confluency (every 3-4 days), the
124 media was removed, cells were washed with 10ml phosphate buffered saline (ThermoFisher,
125 USA), and 2ml of Trypsin-EDTA solution (Gibco, USA) was added to dissociate cells from the
126 flask. To inactivate the trypsin, 8ml of D10 media was added, and cells were pipette-mixed to
127 separate clumps. Culture flasks were re-seeded at a 1:10 ratio which completed one passage.
128 Cells were maintained for no more than 30 passages, so that the integrity of the cell lines was
129 not compromised.

130

131 The optimal sample volume and number of days growth of virus per passage was determined
132 with the Delta variant of concern (VOC) as stated in the Supplementary material section
133 (Supplementary material a. Sample dilution and b. SARS-CoV-2 growth curves).

134

135 **2. Plaque assay**

136 For establishing plaque assay plates, dissociated cell suspension was counted using a
137 Primovert inverted light microscope (ZEISS, Germany) and a disposable C-chip

138 Haemocytometer (NanoEnTek, South Korea), before diluting with D10 media to a
139 concentration of approximately 250,000 cells/ml. Cells were seeded on 24-well culture plates
140 (ThermoFisher, USA) with approximately 500µl of 250,000 cells/ml per well. Plates were
141 incubated at 37°C + 5% CO₂ for 18 hours to produce a confluent monolayer of cells.

142 Media was discarded from all wells, and 190µL of fresh D2 media was added. 10µL of sample
143 was added to the appropriate wells and incubated at 37°C + 5% CO₂ for 1 hour. An overlay
144 solution (prepared by combining equal parts of 2.2% (w/v) Agarose solution (Sigma-Aldrich,
145 USA) and D4 media) was added at 500 µL/well and the plate was incubated at 37°C + 5% CO₂
146 for a further 72 hours. Approximately 1ml/well of Formaldehyde solution (37% w/v) (Merck,
147 Germany) was added, and plates were incubated at room temperature for a minimum of 1
148 hour. The contents of each well were discarded into vermiculite, and plates were stained with
149 crystal violet solution (0.25% w/v in distilled water) for 1 minute, rinsed twice with tap water
150 before air drying and plaque enumeration.

151

152

153 **2. RT-qPCR**

154 For the RT-qPCR assays from Delta and Omicron culture supernatants, RNA was extracted
155 from supernatants using the QiAamp96 Virus Qiacube HT kit (Qiagen, Germany) and RT-qPCRs
156 were run following manufacturer's instruction using TaqPath COVID-19 RT-PCR on a
157 QuantStudio 5 (ThermoFisher, USA). Fluorescence was recorded in the FAM, VIC, ABY and JUN
158 channels for the SARS-CoV-2 ORF1ab, N, and S gene targets, plus MS2 RT-qPCR internal control
159 target respectively. The N gene value was then selected as the most stable target to stratify
160 the samples (lower mean Ct and standard deviation at 10 genome equivalent copies

161 (GCE)/reaction²²). Four and 16 RT-qPCR-confirmed negative samples were also selected as
162 controls in the case of Delta and Omicron clinical samples, respectively. The reproducibility of
163 the RT-qPCR was determined to further inform the Ct difference selected to be indicative of a
164 positive culture by testing 10 replicates from a unique UTM sample at 1X limit of detection
165 (LOD).

166

167 **SARS-CoV-2 clinical sample cohort**

168 Aliquots of universal transport media (UTM, UTM-RT, Copan, USA) (nasopharyngeal samples)
169 from a cohort of adult participants with symptoms suggestive of COVID-19 were collected by
170 the 'Facilitating Accelerated Clinical Evaluation of Novel Diagnostic Tests for COVID -19
171 (FALCON C-19), workstream C (undifferentiated community testing)'. Ethical approval was
172 obtained from the National Research Ethics Service (reference 20/WA/0169) and the Health
173 Research Authority (IRAS ID:28422, clinical trial ID: NCT04408170). Samples were stored at –
174 80°C and thawed for the first time for this study.

175

176 **1. Initial evaluation**

177 The major optimisation experiment was carried out using the Delta variant to compare three
178 chosen detection methods: plaque assay, observable CPE, and comparison of RT-qPCR cycle
179 threshold ²³ values before and after viral culture, in the three cell lines for three passages. All
180 conditions were tested in triplicate. Methods were evaluated for their sensitivity in detecting
181 culture positivity from RT-qPCR positive samples, with the best performer selected for further
182 testing with Omicron samples.

183 **a. Delta clinical samples**

184 Samples were selected from those collected between 19th July 2021 and 26th October 2021,
185 based on a >99% frequency of the Delta variant in the UK between these dates²⁴. Two different
186 sets of Delta virus positive clinical samples were used for Vero E6 and VAT cell lines,
187 respectively (n=36, each set) due to the availability of the cell lines at different time points and
188 the requirement of avoiding using freeze-thawed samples. However, samples were selected
189 for the study based on the Ct value obtained when tested at the time of sample collection
190 using the TaqPath COVID-19 RT-PCR kit (ThermoFisher, United States). Eight samples were
191 selected for each of the following ranges of Ct values: <20, 21-25, 26-30 and >30. Where
192 possible, to ensure a breadth of Ct values within each range, each category was split in half
193 (e.g., <20 was split into 10-15 and 16-20), with four samples taken for each.

194

195 **b. Impact of viral passage on culture positivity**

196 Cells from each cell line were seeded into 24-well culture plates. D2 media was added at
197 190µL/well, and 10µL of each UTM sample was added in triplicate. Plates were incubated at
198 37°C + 5% CO₂ for 2 hours, before a further 200µL/well of D10 media was added. Plates were
199 incubated at 37°C + 5% CO₂ for 72 hours to complete the passage. The process was repeated
200 twice, with 10µL/well being transferred to fresh confluent 24-well plates. Each 72-hour
201 incubation was referred to as a viral passage (giving 3 passages total). After each passage, the
202 culture positivity was determined by the methods detailed above.

203

204 **c. Identification of culture positivity**

205 The three detection methodologies used were microscopy for visual inspection of CPE
206 (supplementary methods C), plaque assay and RT-qPCR.

207 Plaque assays were performed on the 10 μ L of supernatant taken from each well at each
208 passage described in the “Plaque Assay” section. The presence of plaques indicated that
209 infectious virus was present in the well, which was scored as a positive, otherwise wells were
210 scored as negative. Any plates with detached monolayers after staining were repeated.

211 The final detection method to assess viral positivity was a comparison of RT-qPCR cycling
212 threshold ²³ values from a baseline (the original sample diluted 1:40 using D2 media to
213 replicate the dilution factor inherent for viral culture assessment) and the culture supernatant,
214 using the TaqPath RT-qPCR assay. A decrease in Ct value (meaning an increase of viral genetic
215 material) indicates that the virus has successfully replicated and is therefore present and
216 viable. Based on the reproducibility data generated, and that presented in the TaqPath users
217 handbook, we selected a decrease in Ct value of >1 between the baselines and culture
218 supernatant as an indicator of culture positivity.

219 **2. Omicron Variant**

220 **a. Omicron clinical samples**

221 Clinical samples were collected from 14th December 2021- 28th March 2022 based on >99%
222 frequency of Omicron. Samples were also selected based on previous diagnostic results using
223 the Taqpath RT-qPCR kit indicating an S gene target failure^{25,26}. In addition to the clinical
224 samples, an Omicron virus stock (1.4x10⁵pfu/ml) was also incubated in triplicate as a positive
225 control. An aliquot from the same virus stock was heat inactivated at 80°C for 1 hour²⁷ to
226 generate a negative control and UTM media was used as no virus control.

227 **b. Evaluation of optimised culture methodology**

228 The optimized methodology was determined to be a three-day incubation of a single passage,
229 a 1:20 sample dilution, and RT-qPCR based detection. This optimized methodology was
230 validated using 31 positive and 13 negative Omicron samples (Fig. 1). The cell lines Vero E6,
231 VAT and, in addition, hSLAM cells due to high susceptibility for Omicron infection ^{28,29} were
232 used to determine the optimal cell line for this variant. A positive sample (Omicron virus
233 stock), negative sample (inactivated virus stock) and blank (UTM media) were used as controls.

234 **Statistical Analysis**

235 Data were collated and analysed using R v4.1.1 (R Foundation for Statistical Computing,
236 Vienna). Graphical analysis was undertaken using the ggplot package. The coefficient of
237 variation between replicates and the differences between means on Ct values were
238 performed using an independent two-sample T test using R (version 4.2.1)³⁰.

239

240

241

242

243

244

245

246 **RESULTS**

247 Thirty-six nasopharyngeal samples collected during the UK Delta outbreak were used to
248 optimise each methodology. Due to the timings of the experiments and a need to avoid freeze-
249 thaw, different samples were used to assess the Vero E6 and VAT cell lines; however, samples
250 were selected with the same Ct ranges (Fig.S2). There was no significant difference between
251 the mean Ct of the two sample sets (Sample set 1 [Vero E6] mean = 25.34; sample set 2 [VAT]
252 mean = 25.48; p-value = 0.934, CI -3.57 – 3.289). However, the mean Ct of the >30 sample
253 category was higher for sample set 1 than for set 2 (35.51 v. 32.46) and significantly different
254 (p-value = 0.025, CI 0.436-5.667). After evaluating the reproducibility of the RT-qPCR assay,
255 the coefficient of variation calculated at 1X LOD was 0.8%.

256 **Dilution factor**

257 The optimal dilution factor of UTM was assessed to minimise the potential for inhibition or
258 contamination of the cultures without compromising viable virus detection. There was no
259 significant difference in the number of plaques produced with a sample volume of 10 μ L, 20 μ L
260 or 50 μ L within each passage of each cell line (Table S1). However, we did observe signs of
261 contamination in some wells of the 20 μ L and 50 μ L volumes, using both microscopy and visual
262 observation of a change in colour of the media. For these reasons, an optimal input sample
263 volume of 10 μ L (overall dilution = 1:40) was chosen, to reduce the risk of contamination
264 without impacting sensitivity.

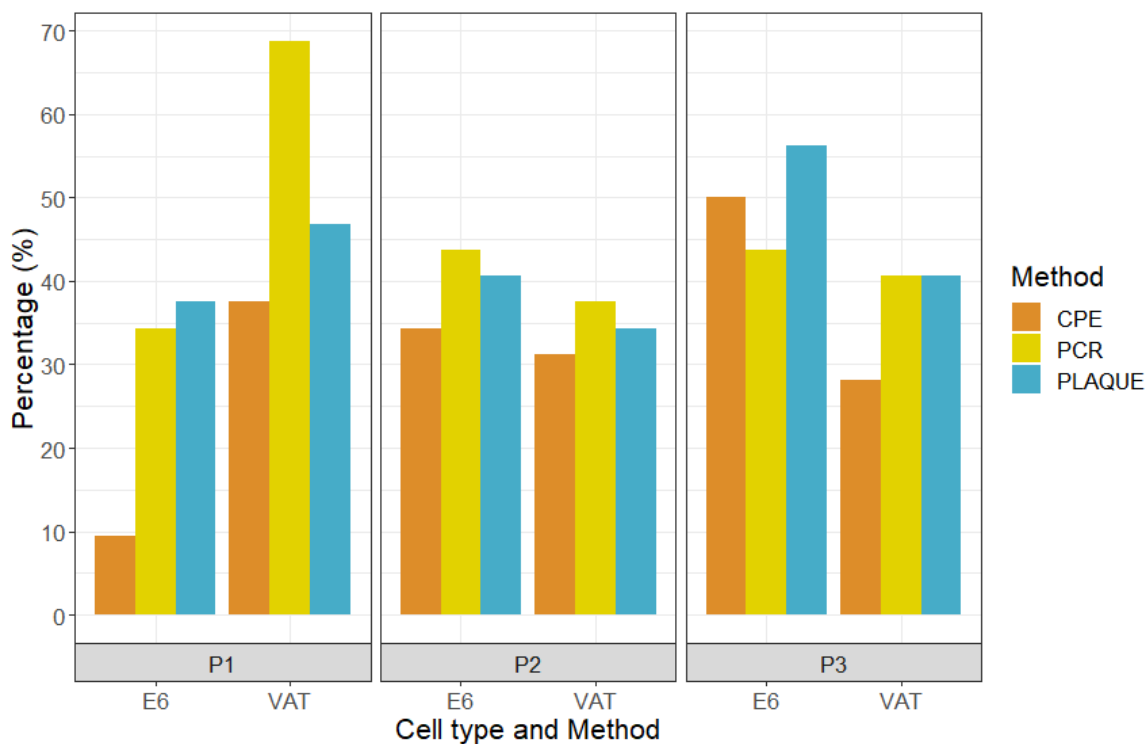
265

266 **Optimisation results**

267 All SARS-CoV-2 positive clinical samples that were tested in triplicate by RT-qPCR produced a
268 valid result. Despite dilution of input clinical samples, contamination was still observed in 14
269 (2.4%) of 576 samples replicates (Table S3A), with 2 and 12 wells contaminated in the E6 and

270 VAT cell line, respectively. In addition, 60 of 576 (13.2%) of the original plaque assays failed
271 due to a lack of viable monolayer and were repeated from a frozen aliquot of the same sample,
272 then added to the final data table (Table S3A). All 60 plaque assay replicate failures were in
273 the E6 cell line.

274 From virus passage 1, the VAT cells resulted in the highest proportion of positive cultures using
275 each detection method (Fig.3). The combination that gave the highest number of positive
276 cultures was RT-qPCR with the VAT cells (68.8%). Whilst further passages improved the
277 positivity rate using Vero E6 cells (34.4%, 43.8% and 43.8% for passages 1, 2 and 3
278 respectively), the sample positivity in VAT cells decreased across the passages (68.8%, 37.5%
279 and 40.6% for passages 1,2 and 3 respectively).



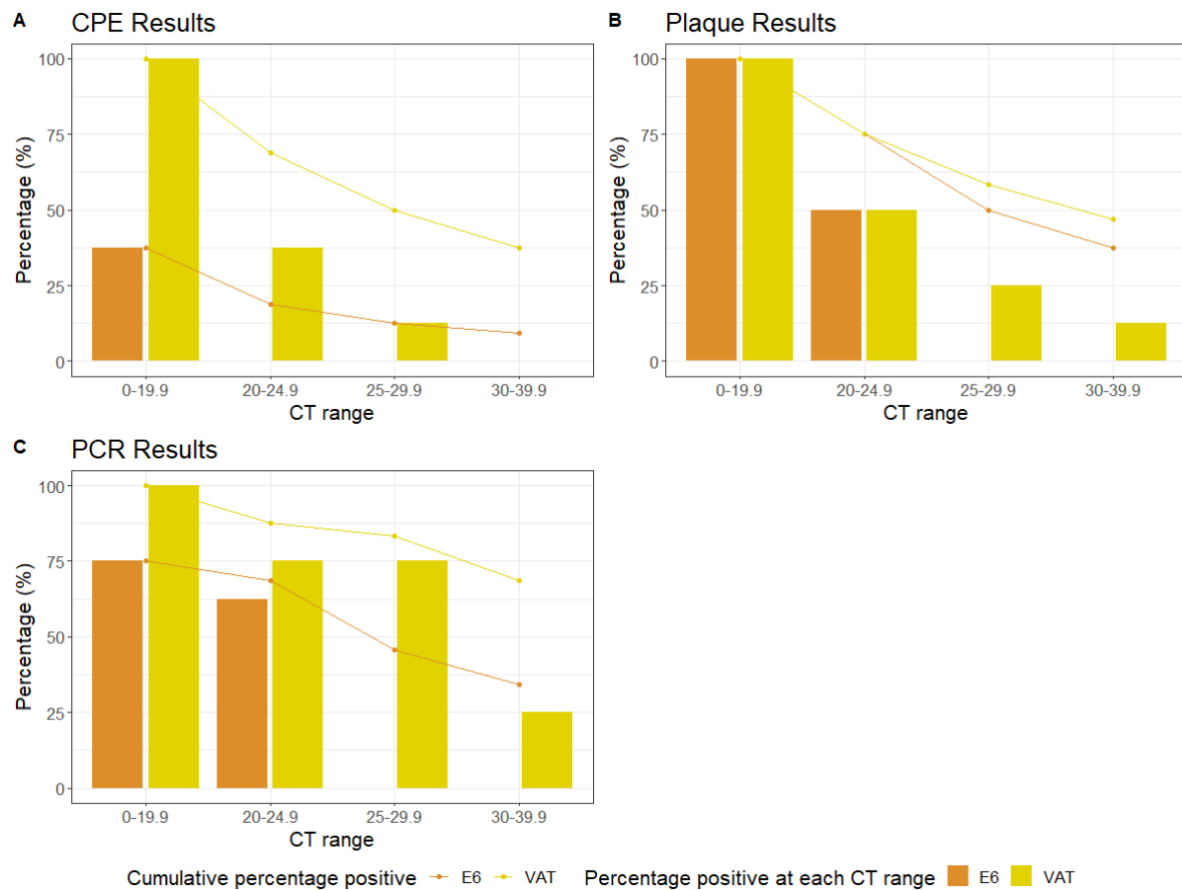
280
281 **Figure 3.** Percentage of positive results by cell type and passage (P1, P2, and P3 refers to
282 passage 1, 2 and 3, respectively) by each detection methodology tested using RT-qPCR
283 positive samples. PCR: RT-qPCR, CPE: cytopathic effect, Plaque: plaque assay.

284

285 For each cell line at virus passage 1, microscopy was the least sensitive detection method. For
286 samples in the <20 Ct range, the use of microscopy to detect CPE yielded a positivity rate of
287 37.5% and 100% in the Vero E6 and VAT cells, respectively. For samples with Ct values in the
288 20 to40 range, the only positives were found in the VAT cells, with a cumulative positivity of
289 50% for all samples <Ct 30 (Fig.4A). There were no positive samples found at any range for
290 Vero E6 cells except for Ct<20 (Table S3A).

291 Plaque assays from culture supernatants identified viable virus in all samples with a Ct <20
292 cycles in both cell lines (Fig.4B). This reduced to 50% in both cell lines for the 20-24.9 Ct range.
293 Cumulative positivity rates for each cell line for samples <Ct 30 were 50% for E6 cells and
294 58.3% for VAT cells. RT-qPCR was the most sensitive detection method for passage 1 (Fig. 4C),
295 particularly when using the VAT cells, which had a cumulative positivity rate of 68.75%, 83.3%
296 87.5%, and 100%, at Ct ranges of and <40, <30, <25, and <20, respectively.

297



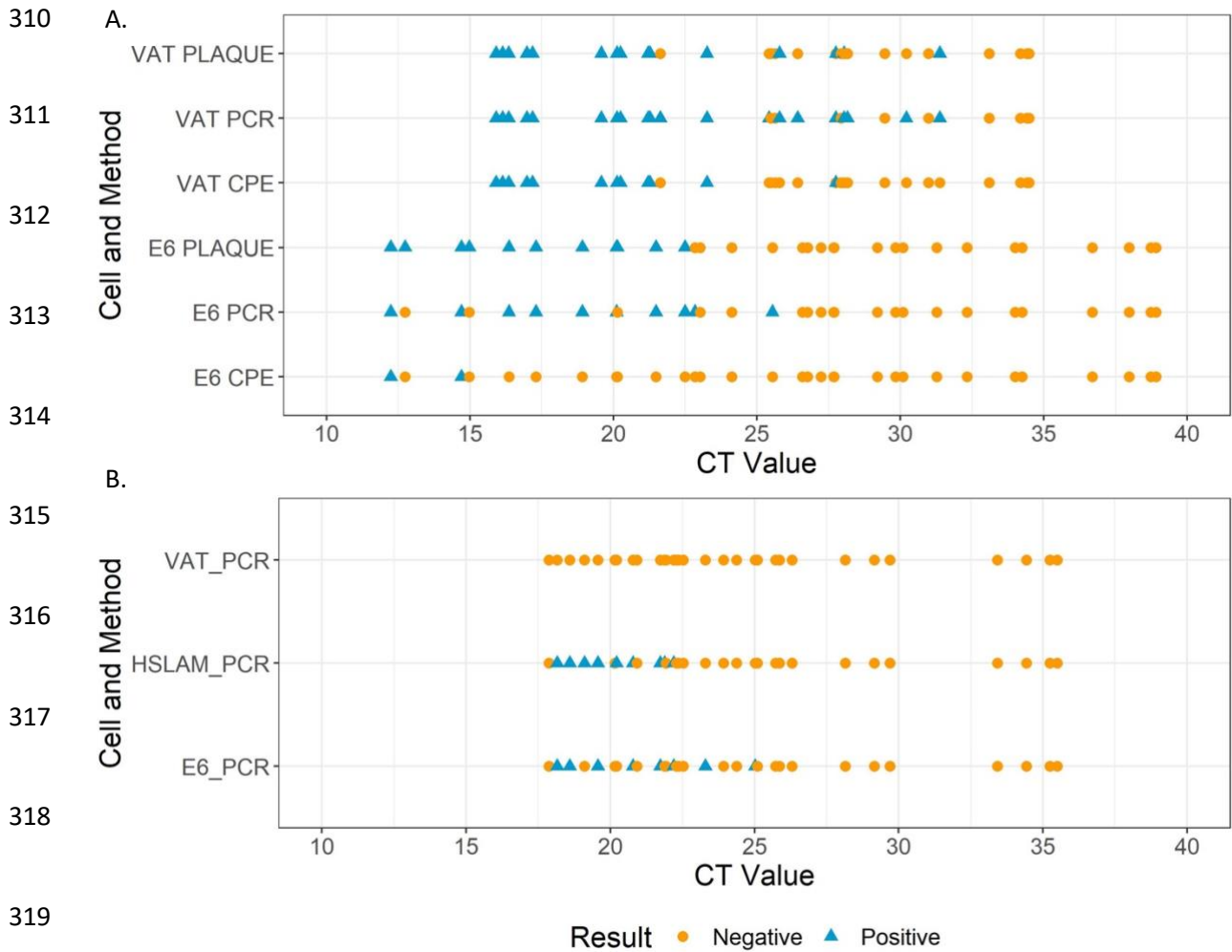
298

299 **Figure 4.** The percentage of positive results according to the different Ct ranges in viral passage
300 1 using the three detection methods. A: cytopathic effect (CPE), B: Plaque assay and C: RT-
301 qPCR.

302

303 The VAT cells were the best performing cell line in terms of sensitivity when using Delta
304 variant-containing samples with lower viral loads (i.e., higher Ct values), with two samples
305 with a Ct >30 identified when RT-qPCR was used as a detection method (sample Cts = 31.79,
306 30.20) (Fig. 5A). The sample with the highest Ct detected by Vero E6 from passage 1 was Ct
307 25.53. The Vero E6 cells with RT-qPCR combination failed to identify two samples below Ct 20,
308 with Cts of 12.74 and 14.97.

309



320 **Figure 5.** Positive and negative results by original Ct values using the different detection
321 methods with A. Delta and B. Omicron samples, respectively. Each dot or triangle represents
322 an individual sample. Most positive results were identified when samples had Ct<25 regardless
323 of the variant used. CPE: cytopathic effect, Plaque: plaque assay and PCR: RT-qPCR.

324
325 Two samples with Ct < 20 (6.25%) assessed with VAT cells failed to produce positive results
326 when microscopy was used as the detection method (Table S3A). The negative control
327 samples were found to be negative by all assays (Table S4), apart from RT-qPCR from VAT cells
328 (1/4 false positive at P3).

329

330 Using the final methodology (10 μ L sample volume, 1 passage of 3 days with VAT cells and RT-
331 qPCR as a detection method) we observed some variation within replicates, particularly with
332 samples with higher Ct values. Of the samples with at least one positive replicate, 67.9% were
333 positive in all replicates, 10.7% in two and 21.4% in one (Table S5).

334

335 **Validation of the final culture protocol using Omicron clinical samples**

336 The optimal protocol from the assay development experiments was determined to be a single
337 three-day incubation of samples with a 1:20 dilution, and RT-qPCR as the detection method.
338 This was then assessed using thirty-one positives and 16 negative samples collected during
339 the Omicron outbreak. Three different cell lines: Vero E6, VAT and hSLAM cells were tested
340 using the same sample set in all cases to assess the optimal cell line for Omicron detection.

341

342 **RT-qPCR analysis of viral P1 samples**

343 Detection of viable virus was demonstrated to be variable across the three cell lines when
344 assessing passaged clinical samples. Using the optimized protocol developed with clinical
345 samples from the Delta wave, the results showed that both hSLAM and Vero E6 cells resulted
346 in a higher proportion of culture positive samples than the VAT cells (Fig. 6), which were
347 unable to isolate replicative virus from any of the samples tested. From the 31 Omicron
348 positives samples used in the study, 7 failed to give a positive result by RT-qPCR in the baseline
349 pre-culture sample after dilution and were therefore treated as negatives. Of the remaining

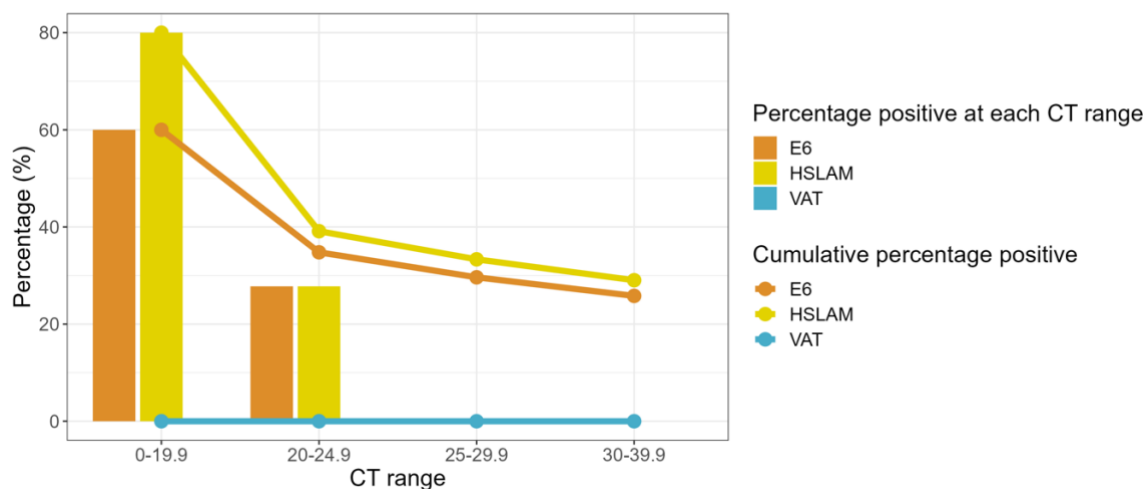
350 samples, 8/24 (33.3%), 9/24 (37.5%) and 0/24 (0%) were positive when cultured with Vero E6,
351 hSLAM and VAT cells, respectively.

352

353 Overall, culture positivity with the hSLAM and Vero E6 cells was 80% and 60% respectively,
354 from samples with a Ct <20 (Fig. 6). In samples with Ct <25, positivity was 35-40% (Fig 5B); no
355 sample with Ct >25 was culture positive in any cell line. (Table S3B). The RT-qPCR negative
356 clinical samples were all found to be negative with the optimized culture protocol (13/13). The
357 positive control (replicating authenticated virus) showed a mean Ct of 17.89, 11.67, and 15.60
358 for Vero E6, hSLAM and VAT cells when cultured, respectively (Table S6). The negative control
359 and no virus controls were negative regardless of the cell line.

360 Again, variation was seen within replicates, particularly with samples with higher Ct values.
361 The best performing cell line, hSLAM, had 69.2% of samples positive in all replicates (Table
362 S5).

363



364

365 **Figure 6.** Percentage of Omicron positive results detected by RT-qPCR according to Ct range.

366 Positive results are presented based on the four different Ct categories for each cell line. Solid
367 coloured lines show the cumulative percentage values for each category.

368

369 **DISCUSSION**

370 The use of cell culture as a virological end point in trials of SARS-CoV-2 therapeutics has been
371 limited compared to molecular approaches, ostensibly due to technical difficulties, lack of
372 standardisation, availability of biosafety level 3 laboratories (BSL3) and reduced sensitivity.
373 However, utilising a culture system to monitor replicating virus could mitigate the potential of
374 molecular methods detecting viral RNA from inactive or lysed viral particles.

375 Here, we have demonstrated that a combination of VAT and hSLAM cells for viral isolation
376 with RT-qPCR of the culture supernatant at passage one for detection is the most sensitive
377 approach for determining the presence of infectious virus of Delta and Omicron VOC,
378 respectively. Culture positivity was higher overall for samples containing the Delta VOC than
379 Omicron, particularly for samples with an RT-qPCR Ct >25.

380 A previous clinical trial of the antiviral drug Molnupiravir utilised a cell culture/supernatant
381 RT-qPCR approach, with Vero E6 cells, and was able to identify replication-competent virus in
382 43.5% of infected participants at enrolment, a significant difference between control and
383 treatment groups at day 3, plus a dose response relationship between the drug and viral
384 isolation⁵. In the case of clinical samples for Delta VOC, we found the VAT cells to be more
385 sensitive than Vero E6 cells for isolating SARS-CoV-2, particularly from samples with lower viral
386 loads. It is generally regarded that the ACE2 receptor expressed by the VAT cells is critical for
387 the entry of SARS-CoV-2 to human epithelial cells, with the serine protease TMPRSS2 priming
388 the S protein for binding³¹. In 2020 the expression of TMPRSS2 by Vero E6 cells has been

389 shown to enhance the isolation of wild-type SARS-CoV-2 from clinical samples³¹, which was
390 also apparent in our results with the Delta variant. However, the lack of Omicron viral
391 replication in any clinical sample with the VAT cells was surprising as there was successful viral
392 infection in VAT cells during the growth curve experiments probably due to cell adaptation
393 (albeit with virus passaged through VAT cells previously), and other studies show Omicron can
394 replicate in VAT cells^{32,33}. This experiment took place in parallel with the other cell lines, and
395 was further repeated to confirm these findings, with the same results obtained. In contrast,
396 we found that Vero E6 and hSLAM cells were much more effective at isolating virus from
397 Omicron samples. Omicron has low efficiency for TMPRSS-2 mediated cell entry and
398 preferentially infects via cathepsin-mediated endocytosis^{29,32}. In addition, it was recently
399 demonstrated that TMPRSS2 activity on both ACE2 and SARS-CoV-2 spike activation is what
400 leads to the significant change in entry requirements from Delta to Omicron lineages³⁴.

401 This study focused on viral isolation in Vero cells and their derivatives and did not assess
402 other cell lines reported to be useful culture systems for SARS-CoV-2. Whilst human
403 epithelium-derived cell lines such as Calu-3 and Caco-2 have been used to isolate and
404 propagate SARS-CoV-2, they produce lower viral titres, do not undergo visible CPE or
405 reproducibly allow viral plaques³⁵, and are less efficient at viral isolation than Vero E6 cells^{36,37}.

406 The use of RT-qPCR to monitor a change in Ct value was found to be more sensitive than
407 microscopy or plaque assay, enabling the detection of replicative virus in the absence of overt
408 CPE. The use of a Ct difference of >1 Ct for culture positivity was selected based on the
409 reproducibility of the assay, and the prediction that RNA from non-replicative virus would
410 decay during incubation, however an increased Ct difference could be selected to increase
411 specificity whilst potentially reducing sensitivity. Due to failed controls on plates (e.g., the

412 virus free control having a disrupted monolayer making result interpretation impossible), the
413 plaque assay approach produced a substantial proportion of unsuccessful replicates, resulting
414 in the need for repeats. While RT-qPCR is the most sensitive and rapid analytical technique
415 used, the data generated require longitudinal analysis to demonstrate the presence of
416 replicating virus.

417 The methodologies reported utilised 24-well microtiter plates to provide a reasonable
418 throughput whilst enabling sufficient inoculum volume to maintain sensitivity. These assays
419 could potentially be carried out in 48 or 96 well plates to maximise throughput or scaled up
420 to 6 well plates or flasks to maximise input volume and potentially sensitivity. Whilst we added
421 antibiotics and antimycotics to cell culture media to reduce contamination, filtering the
422 inoculum could lessen the need for inoculum dilution thereby benefitting sensitivity. Other
423 culture-based methods such as TCID₅₀ assays can be done at a higher throughput than plaque
424 assays, however these were not evaluated during our method development.

425 The specificity of the assay was found to be high, with the only false positives found in passage
426 3 by RT-qPCR for Delta and no false positives for Omicron. This could have been due to
427 contamination of the cell culture or RT-qPCR assays. The study only included four SARS-CoV-2
428 negative swab samples for Delta analysis and further testing is required to assess the test
429 specificity more confidently. In the case of analysis against Omicron clinical samples, a greater
430 number of negative samples were included (n=16).

431 Despite lower sensitivity than RT-qPCR at detecting the presence of SARS-CoV-2 in clinical
432 samples, the greater specificity of cell culture, which only detects viable virus, improves the
433 ability to evaluate efficacy of an antiviral by revealing a larger difference between the
434 treatment and control arms. Infection and viral load kinetics differ between SARS-CoV-2

435 variants, and this work reinforces the need to verify cell line suitability for circulating variants
436 before the selection of cell line for culture-based diagnostics. Even though more effort and
437 caution are required as variations alter, the improved data produced may benefit research
438 projects such as clinical trials.

439 Here we have optimised a cell culture-based assay for determining the presence of infectious
440 SARS-CoV-2 Delta and Omicron variants using clinical nasopharyngeal swabs, determining the
441 optimal sample dilution, culture time, cell line, passage, and detection method. We have also
442 identified an ongoing need to periodically re-assess optimal cell lines throughout the
443 pandemic as the virus evolves and receptor usage and tropism changes over time. This
444 methodology may have application as a secondary virological end point in clinical trials of
445 therapeutics for SARS-CoV-2 in addition to numerous research processes.

446

447 **Funding**

448 The AGILE platform infrastructure is supported by the Medical Research Council (grant
449 number MR/V028391/1) and the Wellcome Trust (grant number 221590/Z/20/Z).

450

451 **Author contributions**

452 BA, TF and TE conceptualised the study. RW, DB, KB, DW, HS, ACA contributed to sample
453 collection during the FALCON study. DW, KB, ARR, VS, TF, and TE contributed to the
454 experimental design and data analysis. DW, KB, ARR, RW, DB, CGB, CT, NK and HS carried out
455 laboratory experiments. Data analysis was carried out by DW, KB, ARR, HS and TE. Funding

456 was received by BG, ERA, SK, TF and TE. DW, KB, ARR, HS, TF and TE wrote the first draft of the
457 manuscript. All authors reviewed and edited the final manuscript.

458

459 **Acknowledgements**

460 Professor Wendy Barclay (Imperial College London) kindly provided the VAT cells. We also wish
461 to acknowledge the CONDOR steering group who lead the FALCON study from which our
462 samples were taken.

463 We acknowledge the support of the National Institute for Health Research (NIHR) Clinical
464 Research Network, which supports delivery of the FALCON study. The views expressed in this
465 article are those of the authors and not necessarily those of the NIHR, or the Department of
466 Health and Social Care.

467 Condor steering group: Dr A. Joy Allen, Dr Julian Braybrook, Professor Peter Buckle, Professor
468 Paul Dark, Dr Kerrie Davis, Professor Adam Gordon, Ms Anna Halstead, Dr Charlotte Harden,
469 Dr Colette Inkson, Ms Naoko Jones, Dr William Jones, Professor Dan Lasserson, Dr Joseph Lee,
470 Dr Clare Lendrem, Dr Andrew Lewington, Mx Mary Logan, Dr Massimo Micocci, Dr Brian
471 Nicholson, Professor Rafael Perera-Salazar, Mr Graham Prestwich, Dr D. Ashley Price, Dr
472 Charles Reynard, Dr Beverley Riley, Professor AJ Simpson, Dr Valerie Tate, Dr Philip Turner,
473 Professor Mark Wilcox, Dr Melody Zhifang.

474

475 **Competing Interest**

476 All authors: no reported conflicts of interest.

477

478 **Correspondence**

479 **Dr Thomas Edwards, email: thomas.edwards@lstm.ac.uk**

480

481 **Supplementary List**

482 **1. Methods**

483 a) Sample dilution

484 b) SARS-CoV-2 growth curves

485 **2. Results**

486 a) Viral growth kinetics for Delta

487 b) Viral growth kinetics for Omicron

488 **Figure S1.** Growth curve of the A. Delta and B. Omicron isolate.

489 **Figure S2.** RT-qPCR Ct values of Delta clinical samples tested by each cell line.

490 **Table S1.** Optimisation of the sample input volume.

491 **Table S2.** RT-qPCR and plaque assay results per cell line for each day with Delta and Omicron viral

492 stocks.

493 Table S3. Total results by cell line for each passage with A. Delta and B. Omicron samples.

494 **Table S4.** Results using Delta negative control samples.

495 **Table S5.** Variation across replicates during the RT-qPCR method in samples with at least one

496 positive replicate.

497 **Table S6.** Results of the Omicron controls used along with the clinical samples.

498

499 **REFERENCES**

- 500 1 Sakamaki, K., Uemura, Y. & Shimizu, Y. Definitions and elements of endpoints in phase III
501 randomized trials for the treatment of COVID-19: a cross-sectional analysis of trials
502 registered in ClinicalTrials.gov. *Trials* **22**, 788 (2021). [https://doi.org/10.1186/s13063-021-](https://doi.org/10.1186/s13063-021-05763-y)
503 [05763-y](https://doi.org/10.1186/s13063-021-05763-y)
- 504 2 Desai, A. & Gyawali, B. Endpoints used in phase III randomized controlled trials of treatment
505 options for COVID-19. **23**, 100403 (2020).
- 506 3 Mehta, H. B., Ehrhardt, S., Moore, T. J., Segal, J. B. & Alexander, G. C. Characteristics of
507 registered clinical trials assessing treatments for COVID-19: a cross-sectional analysis. *BMJ*
508 *Open* **10**, e039978 (2020).
- 509 4 Wang, Y. *et al.* Remdesivir in adults with severe COVID-19: a randomised, double-blind,
510 placebo-controlled, multicentre trial. **395**, 1569-1578 (2020).
- 511 5 Fischer William, A. *et al.* A phase 2a clinical trial of molnupiravir in patients with COVID-19
512 shows accelerated SARS-CoV-2 RNA clearance and elimination of infectious virus. *Science*
513 *Translational Medicine* **14**, eabl7430
- 514 6 Hammond, J. *et al.* Oral Nirmatrelvir for High-Risk, Nonhospitalized Adults with Covid-19. *N*
515 *Engl J Med* **386**, 1397-1408 (2022).
- 516 7 Kevadiya, B. D. *et al.* Diagnostics for SARS-CoV-2 infections. **20**, 593-605 (2021).
- 517 8 Singanayagam, A. *et al.* Duration of infectiousness and correlation with RT-PCR cycle
518 threshold values in cases of COVID-19, England, January to May 2020. *Eurosurveillance* **25**,
519 2001483 (2020). [https://doi.org/doi:https://doi.org/10.2807/1560-](https://doi.org/doi:https://doi.org/10.2807/1560-7917.ES.2020.25.32.2001483)
520 [7917.ES.2020.25.32.2001483](https://doi.org/doi:https://doi.org/10.2807/1560-7917.ES.2020.25.32.2001483)
- 521 9 van Kampen, J. J. A. *et al.* Duration and key determinants of infectious virus shedding in
522 hospitalized patients with coronavirus disease-2019 (COVID-19). **12**, 267 (2021).
- 523 10 Cevik, M. *et al.* SARS-CoV-2, SARS-CoV, and MERS-CoV viral load dynamics, duration of viral
524 shedding, and infectiousness: a systematic review and meta-analysis. *The lancet microbe* **2**,
525 e13-e22 (2021).
- 526 11 Wurtz, N., Penant, G., Jardot, P., Duclos, N. & La Scola, B. Culture of SARS-CoV-2 in a panel of
527 laboratory cell lines, permissivity, and differences in growth profile. *European Journal of*
528 *Clinical Microbiology & Infectious Diseases* **40**, 477-484 (2021).
529 <https://doi.org/10.1007/s10096-020-04106-0>
- 530 12 Wei, J. *et al.* Genome-wide CRISPR screens reveal host factors critical for SARS-CoV-2
531 infection. *Cell* **184**, 76-91. e13 (2021).
- 532 13 Murgolo, N. *et al.* SARS-CoV-2 tropism, entry, replication, and propagation: Considerations
533 for drug discovery and development. *PLoS Pathogens* **17**, e1009225 (2021).
534 <https://doi.org/10.1371/journal.ppat.1009225>
- 535 14 Leonard, V. H. J., Hodge, G., Reyes-Del Valle, J., McChesney, M. B. & Cattaneo, R. Measles
536 virus selectively blind to signaling lymphocytic activation molecule (SLAM; CD150) is
537 attenuated and induces strong adaptive immune responses in rhesus monkeys. *Journal of*
538 *virology* **84**, 3413-3420 (2010).
- 539 15 Rihn, S. J. *et al.* A plasmid DNA-launched SARS-CoV-2 reverse genetics system and
540 coronavirus toolkit for COVID-19 research. *PLoS Biology* **19**, e3001091 (2021).
- 541 16 Prince, T. *et al.* Analysis of SARS-CoV-2 in Nasopharyngeal Samples from Patients with COVID-
542 19 Illustrates Population Variation and Diverse Phenotypes, Placing the Growth Properties of

- 543 Variants of Concern in Context with Other Lineages. *mSphere*, e0091321 (2022).
544 <https://doi.org/10.1128/msphere.00913-21>
- 545 17 Matsuyama, S. *et al.* Enhanced isolation of SARS-CoV-2 by TMPRSS2-expressing cells.
546 *Proceedings of the National Academy of Sciences* **117**, 7001-7003 (2020).
547 <https://doi.org/10.1073/pnas.2002589117>
- 548 18 Folgueira, M. D., Luczkowiak, J., Lasala, F., Pérez-Rivilla, A. & Delgado, R. Prolonged SARS-
549 CoV-2 cell culture replication in respiratory samples from patients with severe COVID-19.
550 *Clinical microbiology and infection : the official publication of the European Society of Clinical*
551 *Microbiology and Infectious Diseases* **27**, 886-891 (2021).
- 552 19 Berengua, C. *et al.* Viral culture and immunofluorescence for the detection of SARS-CoV-2
553 infectivity in RT-PCR positive respiratory samples. *Journal of clinical virology : the official*
554 *publication of the Pan American Society for Clinical Virology* **152**, 105167-105167 (2022).
- 555 20 Mendoza, E. J., Manguiat, K., Wood, H. & Drebot, M. Two Detailed Plaque Assay Protocols for
556 the Quantification of Infectious SARS-CoV-2. *Curr Protoc Microbiol* **57**, ecpmc105-ecpmc105
557 (2020). <https://doi.org/10.1002/cpmc.105>
- 558 21 Craig, N. *et al.* Direct Lysis RT-qPCR of SARS-CoV-2 in Cell Culture Supernatant Allows for Fast
559 and Accurate Quantification. *Viruses* **14**, 508 (2022).
- 560 22 Biosystems, A. TaqPath™ COVID-19 Combo Kit INSTRUCTIONS FOR USE. (2020).
- 561 23 Tchesnokova, V. *et al.* Acquisition of the L452R mutation in the ACE2-binding interface of
562 Spike protein triggers recent massive expansion of SARS-Cov-2 variants. *Journal of clinical*
563 *microbiology* **59**, e00921-00921 (2021).
- 564 24 Hodcroft, E. e. a. *CoVariants- Overview of Variants/Mutations*, <[https://covariants.org/per-](https://covariants.org/per-variant)
565 [variant](https://covariants.org/per-variant)> (
- 566 25 Li, A., Maier, A., Carter, M. & Guan, T. H. Omicron and S - gene target failure cases in the
567 highest COVID - 19 case rate region in Canada–December 2021. *Journal of medical virology*
568 **94**, 1784 (2022).
- 569 26 Metzger, C. M. *et al.* PCR performance in the SARS-CoV-2 Omicron variant of concern? *Swiss*
570 *medical weekly* **151**, w30120-w30120 (2021).
- 571 27 Patterson, E. I. *et al.* Methods of inactivation of SARS-CoV-2 for downstream biological
572 assays. *The Journal of infectious diseases* **222**, 1462-1467 (2020).
- 573 28 Pawar, S. D. *et al.* Replication of SARS-CoV-2 in cell lines used in public health surveillance
574 programmes with special emphasis on biosafety. *Indian Journal of Medical Research* **155**,
575 129-135 (2022).
- 576 29 Dighe, H. *et al.* Differential cell line susceptibility to the SARS-CoV-2 omicron BA. 1.1 variant
577 of concern. *Vaccines* **10**, 1962 (2022).
- 578 30 R Core Team, R. R: A language and environment for statistical computing. (2013).
- 579 31 Hoffmann, M. *et al.* SARS-CoV-2 Cell Entry Depends on ACE2 and TMPRSS2 and Is Blocked by
580 a Clinically Proven Protease Inhibitor. *Cell* **181**, 271-280.e278 (2020).
581 <https://doi.org/10.1016/j.cell.2020.02.052>
- 582 32 Meng, B. *et al.* Altered TMPRSS2 usage by SARS-CoV-2 Omicron impacts infectivity and
583 fusogenicity. *Nature* **603**, 706-714 (2022).
- 584 33 Saito, A. *et al.* Virological characteristics of the SARS-CoV-2 Omicron BA. 2.75 variant. *Cell*
585 *host & microbe* **30**, 1540-1555. e1515 (2022).
- 586 34 Aggarwal, A. *et al.* TMPRSS2 activation of Omicron lineage Spike glycoproteins is regulated by
587 TMPRSS2 cleavage of ACE2. *bioRxiv*, 2023.2009. 2022.558930 (2023).
- 588 35 Mautner, L. *et al.* Replication kinetics and infectivity of SARS-CoV-2 variants of concern in
589 common cell culture models. **19**, 76 (2022).
- 590 36 Essaidi-Laziosi, M. *et al.* Estimating clinical SARS-CoV-2 infectiousness in Vero E6 and primary
591 airway epithelial cells. *The Lancet Microbe* **2**, e571 (2021).
- 592 37 Funnell, S. G. *et al.* A cautionary perspective regarding the isolation and serial propagation of
593 SARS-CoV-2 in Vero cells. *NPJ vaccines* **6**, 83 (2021).

